Published in Contributions to Mineralogy and Petrology 115, issue 3, 287-302, 1994
which should be used for any reference to this work

Petrology and geochronology of eclogites from the Variscan Schwarzwald (F.R.G.)

Angelika Kalt[1], Michael Hanel[2]*, Helmut Schleicher[2]*, and Ulrich Kramm[3]

[1] Institut für Petrographie und Geochemie, Universität Karlsruhe, Kaiserstrasse 12, D-76128 Karlsruhe, Germany
[2] Mineralogisch-Petrographisches Institut, Universität Freiburg, Albertstrasse 23b, D-79104 Freiburg, Germany
[3] Institut für Mineralogie, Universität Münster, Corrensstrasse 24, D-48149 Münster, Germany

Abstract. The Moldanubian basement of the Schwarzwald contains basic to ultrabasic rocks of both crustal and mantle origin which display high-pressure mineral assemblages or relics of such. In order to constrain the P-T-t evolution of the crustal high-pressure rocks, petrological and geochronological studies have been carried out on three eclogite samples. Geothermobarometric estimations indicate minimum metamorphic pressures of 1.6 GPa and equilibration temperatures of 670–750°C. Reaction textures document various metamorphic stages during exhumation of the high-pressure rocks. The age of high-pressure metamorphism is constrained by Sm-Nd isochrons of 332 ± 13 Ma, 334 ± 11 Ma, and 337 ± 6 Ma defined by garnet, whole rock and clinopyroxene. For one sample, large garnets show prominent growth zoning in terms of major elements, Sm, Nd, and inclusions, dividing the grains into two growth stages. Sm-Nd isotope analyses on these garnets indicate that the time span between the two growth stages is too small to be resolved, reflecting a rather rapid metamorphic evolution. This result is further constrained by a Rb-Sr isochron age of 325 ± 6 Ma on retrograde biotite and whole rock on the same sample. For one of the studied eclogites, formation of the magmatic precursor rocks is possibly approximated by the Ordovician U-Pb upper intercept age of a discordia from zircons.

Introduction

High-pressure rocks are often found intercalated in medium to high-grade metamorphic terrains as basement inliers of variable size and shape, generally anisofacial to their host rocks. Within the Variscan belt, these rocks are frequently found in the Moldanubian zone (for a review see O'Brien et al. 1990) for which a complex structural and metamorphic evolution during the Palaeozoic is to be inferred (Franke 1989). As high-pressure rocks give evidence of crustal thickening and possibly of palaeoplate sutures, as in the case of eclogites, they can be the key to unravelling the geological histories of complex metamorphic terrains such as the Moldanubian.

If high-pressure mineral assemblages and mineral compositions survived retrogression during uplift, a number of geothermometers and geobarometers can serve to estimate the peak P-T conditions during metamorphism (Carswell and Harley 1990), allowing for conclusions on burial depth and crustal thickness. By the same means, if the conditions of retrogression can also be determined, then P-T paths for the high-pressure rocks can be set up (e.g. O'Brien 1989; O'Brien et al. 1992), providing important constraints on tectonic and thermal models for collision zones.

Information on subduction and collision processes is complete only when the age of high-pressure metamorphism is determined. Several dating methods have been applied to eclogites and other high-pressure rocks with varying success. K-Ar and Rb-Sr dating techniques are only applicable to rocks containing phengite, paragonite or amphibole and bear the problems of the presence of excess argon and of being sensitive to resetting by temperature elevation. U-Pb dating of zircons is afflicted with interpretatory problems resulting from only insufficient petrological control on accessory phases and should therefore be used only in conjunction with other dating techniques.

The Sm-Nd method has proven to be appropiate for dating high-pressure metamorphism (Jagoutz 1988; Mørk et al. 1988; Stosch and Lugmair 1990; Jamtveit et al. 1991; Beard et al. 1992) as the main high-pressure phases garnet and clinopyroxene are used and as the Sm-Nd system is not easily reset by temperature elevation. Nevertheless, there are still basic problems to the interpretation of Sm-Nd data from high-pressure rocks, namely the difficulty of connecting P-T data established on major element distributions to isotope data based on trace element decay systems, insufficient data on diffusion velocities of Sm and Nd in garnet and clinopyrox-

* *Present address:* Mineralogisch-Petrographisches Institut, Universität Heidelberg, Im Neuenheimer Feld 236, D-69120 Heidelberg, Germany

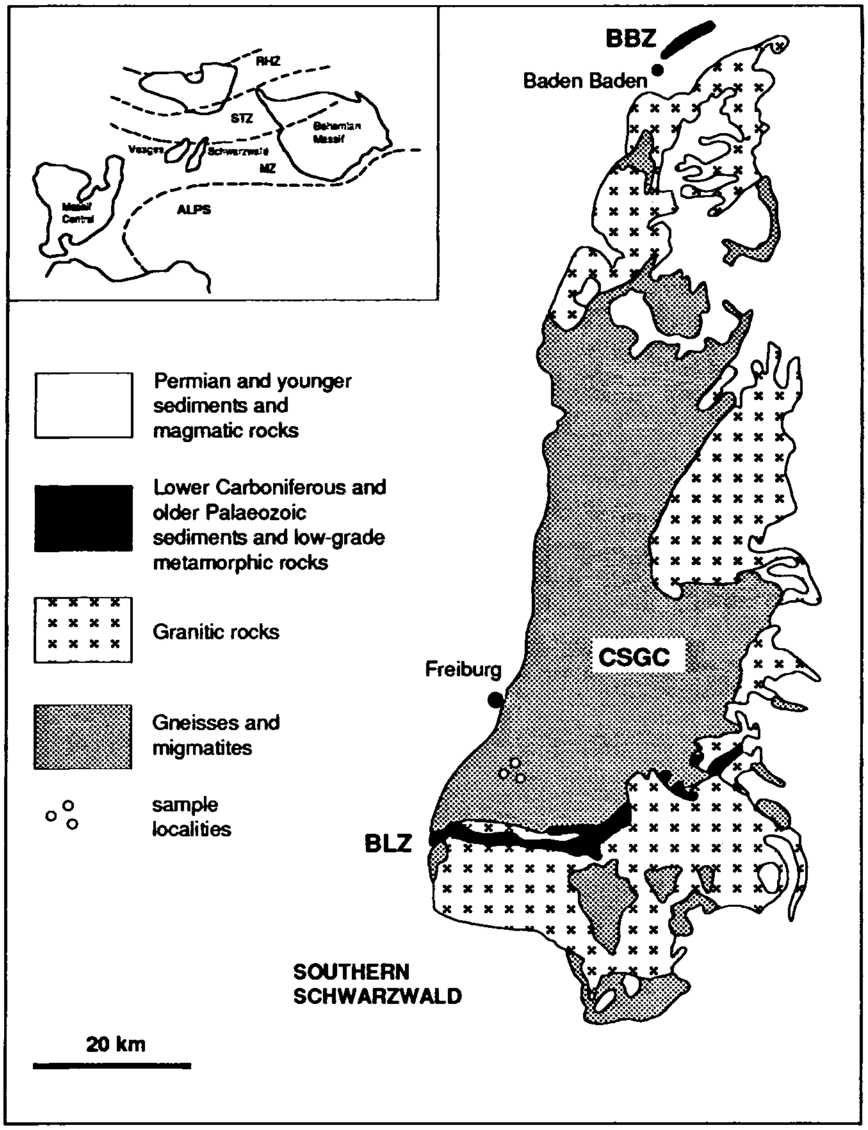

Fig. 1. Simplified geological map of the Schwarzwald (based on Wickert and Eisbacher 1988 and Wimmenauer and Stenger 1989) showing the main basement units as well as the sample localities. Abbreviations are: *BBZ:* Baden-Baden Zone; *BLZ:* Badenweiler-Lenzkirch Zone; *CSGC:* Central Schwarzwald Gneiss Complex. The *inset* shows the Schwarzwald within the Variscan setting. Abbreviations are: *RHZ:* Rhenohercynian Zone; *STZ:* Saxothuringian Zone; *MZ:* Moldanubian Zone

ene, and the lack of control on closure temperatures in general.

Hence, the objective of this paper must be twofold. The primary intention is to present new mineralogical, petrological and geochronological data on eclogites of the Moldanubian part of the Schwarzwald in order to provide constraints on the tectonometamorphic evolution. The second intention, emerging from the application of different dating techniques is to focus on general problems in dating high-pressure rocks.

Geological setting

The Schwarzwald in southwestern Germany covers part of the Moldanubian and Saxothuringian zones of the Variscan orogenic belt (Fig. 1). Its largest basement unit, the Central Schwarzwald Gneiss Complex (CSGC, Krohe and Eisbacher 1988) is a Moldanubian nappe pile. During Variscan convergence, the CSGC was tectonically emplaced over low to medium-grade metamorphic rocks of the Saxothuringian zone to the north as well as over volcanic and sedimentary sequences and low-grade metamorphic series to the south (Eisbacher et al. 1989). Further to the south, the latter units are bordered by the crystalline basement rocks of the Southern Schwarzwald. Numerous granitoids intruded both the metamorphic rocks of the CSGC and of the Southern Schwarzwald.

The CSGC is dominated by monotonous metapsammitic to metapelitic gneisses which are locally disrupted by variegated metasedimentary gneiss series and by meta-igneous gneisses (Wimmenauer et al. 1989). The predominant metamorphic overprint of all these rocks is of the low-pressure high-temperature type (LP-HT). Migmatization in the monotonous gneisses is fairly widespread, the P-T conditions being estimated at 675–690°C and 0.4–0.5 GPa by Mehnert and Büsch (1982).

The monotonous gneisses and migmatites bear mostly lens-shaped bodies of mafic and minor ultramafic rocks showing high-pressure mineral assemblages or relics of such. Apart from minor mantle-derived ultramafic bodies the high-pressure rocks are eclogites with the primary paragenesis grt + omph ± rut ± qtz ± ky ± amph ± cz. As most of the eclogites are strongly retrogressed only a minimum estimate of the peak metamorphic conditions of 560–650° and 10 kb was given by Klein and Wimmenauer (1984).

Evidence from structural geology suggests the first stage common to both high-pressure rocks and encompassing LP-HT gneisses to be a postmigmatitic HT deformation (Flöttmann and Kleinschmidt 1989). Up to that stage the metamorphic evolution of the two rock types was probably separate, although there are clear examples of a common HT overprint of HP rocks and their host rocks and a few of the surrounding gneisses even seem to bear relics of a former high-pressure stage (Wimmenauer and Stenger 1989).

Geochronological studies in the Schwarzwald have mainly focussed on dating the intrusion of granitic rocks (335–310 Ma; Brewer and Lippolt 1974; Wendt et al. 1974; Todt 1976). In contrast, P-T paths and geochronology of the different metamorphic rock types of the CSGC and of the Southern Schwarzwald are not very well constrained. U-Pb ages of monazites from migmatites and monotonous gneisses as well as the results of Rb-Sr thin-slab dating on migmatites indicate a Lower Carboniferous age of LP-HT metamorphism, including migmatization (336–330 Ma; Kalt et al. 1993). On the other hand, U-Pb analyses of zircons as well as Rb-Sr whole rock studies on different metamorphic rocks point to magmatic and metamorphic events between 520 and 470 Ma (Hofmann and Köhler 1973; Steiger et al. 1973; Todt and Büsch 1981; Kober 1986, 1987) that cannot clearly be defined due to the lack of petrological constraints.

Petrography and mineral chemistry

All samples were collected from outcrops near the southern margin of the CSGC (Fig. 1) where the surrounding gneisses were extensively migmatized.

Sample Lo-1

Sample Lo-1 was taken from a dm-sized lens of eclogite enclosed in LP-HT gneisses that lack any relics of high-pressure metamorphism. The eclogite is a macroscopically homogeneous, texturally isotropic, dark-coloured and fine-grained rock. Garnet and clinopyroxene are the major phases. Amphibole, magnetite, plagioclase and ilmenite are present as minor phases whereas rutile, sphene and apatite are accessory minerals.

Garnets are unzoned and Fe-rich (Table 1). They contain inclusions of cpx and rutile. Many garnets are surrounded by thin rims of plagioclase (An_{63-70}), magnetite, ilmenite, rutile (in places overgrown by sphene) and amphibole. Rutile and garnet are consumed by plagioclase and ilmenite, pointing to the reaction grt + rut = ilm + plg (+ sph). More rarely, radiating kelyphites of plagioclase (An_{50-60}) and amphibole are observed around garnet.

Clinopyroxene (cpxI) forms small inclusions in garnet as well as anhedral grains in the matrix. Whereas cpxI inclusions in garnet have rather uniform compositions ($X_{jad} = 0.32$–0.39), cpxI grains in the groundmass are zoned with X_{jad} decreasing from core (0.39) to rim (0.22). CpxI groundmass grains show abundant inclusions of rutile and rarely of clinozoisite. Their rims are partly transformed to vermicular intergrowths of plagioclase (An_{15-20}) and Fe-rich diopside (cpxII).

Sample Z-48

Sample Z-48 was collected from a large body of approximately 10 m in diameter, enclosed in migmatic rocks. Contacts to the migmatites are not exposed. The rocks are medium to coarse-grained and very heterogeneous on a small scale. Two textural and compositional varieties can be distinguished. Most parts of the body are retrogressed eclogites that contain abundant garnet, symplectite consisting of pyroxene and plagioclase, kyanite, quartz and amphibole, as well as rutile, sphene, zircon and apatite as accessory phases. These eclogitic domains grade into other parts of the body that are very rich in garnet (up to 2 cm in diameter) and quartz and almost devoid of symplectite and amphibole. Apart from garnet and quartz, these parts of the rock contain kyanite, plagioclase, orthopyroxene and amphibole as minor phases as well as rutile, sphene, zircon, apatite and sillimanite as accessory phases. Both rock types may in parts contain biotite, sometimes intergrown with plagioclase (± quartz, ± sillimanite). The chemical components required for the formation of these retrograde phases have been introduced into the rock by fluids at a very late stage of metamorphism.

Although the outcrop shows two textural and compositional varieties, mineral compositions throughout sample Z-48 are fairly uniform. Garnets larger than about 2 mm in diameter show zoning, corresponding to a macroscopically discernible change in colour. Zoning is characterized by complementary profiles for Fe and Mg (Fig. 2a), dividing garnets into three distinct zones: (1) a reddish-coloured core that is Fe-rich and Mg-poor and shows a plateau for Ca as well as the highest Mn contents; (2) an inner, pink-coloured rim, characterized by high Mg and decreased Fe and Mn contents, a peak in Ca and subsequently strongly decreasing Ca contents; (3) an outermost rim showing a strong decrease in Mg and a complementary increase in Fe. In garnets smaller than about 2 mm in diameter only zones 2 and 3 can be observed (Fig. 2b) which in terms of composition correspond very well to those of the large garnets.

Division of the large garnets into distinct zones is confirmed by the nature and distribution of inclusions observed within the garnets although the latter could also partly be due to a slower radial growth rate as garnet supply stayed constant: the cores have abundant inclusions of quartz, rutile, and pargasite (Table 1) and rarely of kyanite, whereas the inner rims are either devoid of inclusions or have only very few inclusions of the same minerals. Contacts of quartz, rutile and pargasite towards garnet are stable; kyanite is surrounded by fine-grained coronas (see below). In one garnet core, pargasites contain inclusions of staurolite (Table 1) and of tiny spinel grains. The largest staurolite grain is in contact with pargasite on one side and with garnet on the other. It shows zoning with X_{Mg} decreasing from core (0.40) to rim (0.20) and has inclusions of spinel and rutile. X_{Mg} of the adjacent garnet is 0.48, X_{Mg} of the bordering pargasite is 0.68. Smaller staurolite grains all have X_{Mg} values of about 0.20–0.26, so that in all cases $X_{Mg}(stt) < X_{Mg}(grt) < X_{Mg}(parg)$.

Garnets within the eclogitic parts of the rock are frequently rimmed by kelyphites consisting of plagioclase (An_{85-95}), amphibole (gedrite or hornblende) and/or orthopyroxene (Table 1), partly with spinel. In places where garnet was in contact with quartz, seams of plagioclase (variable composition) towards garnet and of orthopyroxene (Table 1) and/or amphibole towards quartz can be observed. In the quartz-rich parts of the rock, there are also a few metastable contacts between garnet and quartz.

Fine-grained symplectites consisting of plagioclase (An_{25-35}) and clinopyroxene or orthopyroxene (Table 1) indicate the former presence of omphacite. These symplectites may be further replaced by hornblende. Kyanite is only preserved as relics within very fine-grained coronas of hercynite and anorthite, in cases also sericite. This transformation requires a supply of Mg, Fe and Ca. As kyanites and their surrounding coronas are either embedded in symplectites, located between garnet grains or even included in garnet, Mg, Fe and Ca were most likely supplied during retrogression of garnet and omphacite.

Minor and accessory phases are rutile, included in garnet cores, zircon in garnet rims and in the matrix as well as apatite, sphene and magnetite and ilmenite in the matrix.

Sample Alp-1

Sample Alp-1 comes from an isolated cliff of eclogite. The rock is of dark greenish-grey colour. It is heterogeneous in terms of grain size and mode. Main minerals are clinopyroxene, amphibole and garnet. Quartz as well as kyanite are minor phases and accessory minerals are rutile, apatite and zircon. The texture is isotropic and inequigranular with clinopyroxenes and amphiboles being the largest grains.

Table 1. Mineral compositions

	Z-48									Lo-1					Alp-1			
	grt core	grt inner rim	grt outer rim	stt in grt	parg in grt	amph in kel	amph in sym	opx in sym, kel	cpx in sym	grt core	grt rim	cpx I core	cpx I rim	amph in sym	grt core	grt rim	cpx	amph
SiO_2	37.80	40.70	40.28	27.01	41.28	42.04	51.88	52.89	53.72	38.55	38.40	54.41	52.99	42.87	38.35	38.13	53.39	43.78
TiO_2	0.04	0.05	0.08	0.93	0.20	0.04	0.34	0.05	0.05	0.04	0.09	0.09	0.26	0.54	0.08	0.08	0.13	0.41
Cr_2O_3	0.00	0.13	0.10	0.22	0.71	0.40	0.13	0.00	0.17	0.02	0.01	0.03	0.00	0.03	0.02	0.04	0.01	0.08
Al_2O_3	20.83	22.67	22.35	54.40	19.71	18.10	5.56	1.84	1.17	21.03	21.15	7.72	7.21	12.01	20.62	20.67	4.43	12.40
Fe_2O_3	0.70	0.71	0.00	n.c.	0.00	0.76	0.42	1.21	1.28	1.91	1.52	3.36	1.91	2.68	3.02	2.72	2.10	2.17
FeO	27.45	15.24	19.72	10.54	13.34	14.83	7.11	18.83	3.80	21.11	21.78	3.11	6.43	11.50	19.64	22.79	5.04	12.94
MnO	1.96	0.16	0.23	0.03	0.10	0.18	0.05	0.18	0.07	0.32	0.24	0.04	0.14	0.11	0.22	0.25	0.00	0.07
MgO	4.04	14.32	11.91	4.89	10.01	17.63	18.52	24.67	15.57	5.13	5.09	9.64	10.21	13.53	5.71	5.73	12.08	11.36
NiO	n.a.	n.a.	n.a.	n.a.	n.a.	n.a.	n.a.	n.a.	n.a.	n.a.	n.a.	n.a.	n.a.	n.a.	n.a.	n.a.	n.a.	n.a.
CaO	6.64	5.97	5.14	0.01	10.81	0.79	12.26	0.51	23.81	11.96	11.56	16.34	17.13	11.48	12.34	9.65	20.04	12.61
Na_2O	0.02	0.03	0.05	0.00	1.47	2.33	0.83	0.02	0.47	0.04	0.01	5.15	3.63	2.66	0.02	0.00	2.53	2.06
K_2O	0.00	0.00	0.00	0.00	0.36	0.00	0.03	0.04	0.00	0.01	0.02	0.00	0.01	0.42	0.00	0.02	0.00	0.03
H_2O					2.06	2.08	2.12							2.03				2.03
Total	99.47	100.00	99.86	98.06	100.04	99.19	99.26	99.99	100.10	100.14	100.17	99.88	99.94	99.85	100.01	100.07	99.74	99.95
Si	3.003	2.993	3.017	7.396	6.015	6.066	7.355	1.942	1.970	2.985	2.983	1.968	1.940	6.333	2.968	2.968	1.962	6.456
Ti	0.002	0.003	0.005	0.192	0.022	0.004	0.036	0.001	0.001	0.002	0.006	0.003	0.007	0.060	0.005	0.005	0.004	0.046
Cr	0.000	0.008	0.006	0.045	0.082	0.046	0.014	0.000	0.005	0.001	0.001	0.001	0.000	0.004	0.001	0.002	0.000	0.010
Al	1.951	1.965	1.973	17.553	3.385	3.077	0.929	0.080	0.051	1.920	1.936	0.329	0.311	2.088	1.880	1.896	0.192	2.154
Fe^{3+}	0.042	0.040	0.000	0.000	0.000	0.083	0.045	0.034	0.035	0.111	0.089	0.092	0.053	0.298	0.176	0.159	0.058	0.241
Fe^{2+}	1.824	0.938	1.235	2.413	1.625	1.789	0.843	0.578	0.117	1.367	1.415	0.094	0.197	1.420	1.271	1.483	0.155	1.596
Mn	0.132	0.010	0.015	0.007	0.012	0.022	0.006	0.006	0.002	0.021	0.016	0.001	0.004	0.014	0.015	0.016	0.000	0.009
Mg	0.478	1.570	1.330	1.995	2.173	3.792	3.913	1.350	0.851	0.592	0.589	0.519	0.557	2.977	0.659	0.665	0.661	2.498
Ca	0.566	0.471	0.413	0.002	1.687	0.122	1.861	0.009	0.935	0.992	0.962	0.633	0.672	1.814	1.023	0.805	0.789	1.993
Na	0.003	0.004	0.007	0.013	0.416	0.651	0.228	0.000	0.033	0.006	0.002	0.361	0.258	0.760	0.002	0.000	0.180	0.588
K	0.000	0.001	0.000	0.000	0.067	0.004	0.006	0.000	0.000	0.001	0.002	0.000	0.001	0.079	0.000	0.002	0.000	0.005
OH					2.000	2.000	2.000							2.000				2.000
Total	8.000	8.000	8.000	29.615	15.482	15.655	15.237	4.000	4.000	8.000	8.000	4.000	4.000	15.846	8.000	8.000	4.000	15.594
X_{Mg}	0.208	0.626	0.518	0.453	0.572	0.679	0.823	0.700	0.880	0.302	0.294	0.847	0.739	0.677	0.342	0.309	0.810	0.610

Calculations: garnet: 8 cations and 12 oxygens, pyroxene: 4 cations and 6 oxygens, amphibole: 15 cations + Na + K and 22 oxygens + 2 OH, staurolite: 46 oxygens
Abbreviations: kel: kelyphite around garnet, sym: symplectite of cpx and plg after omphacite, n.a.: not analyzed, n.c.: not calculated

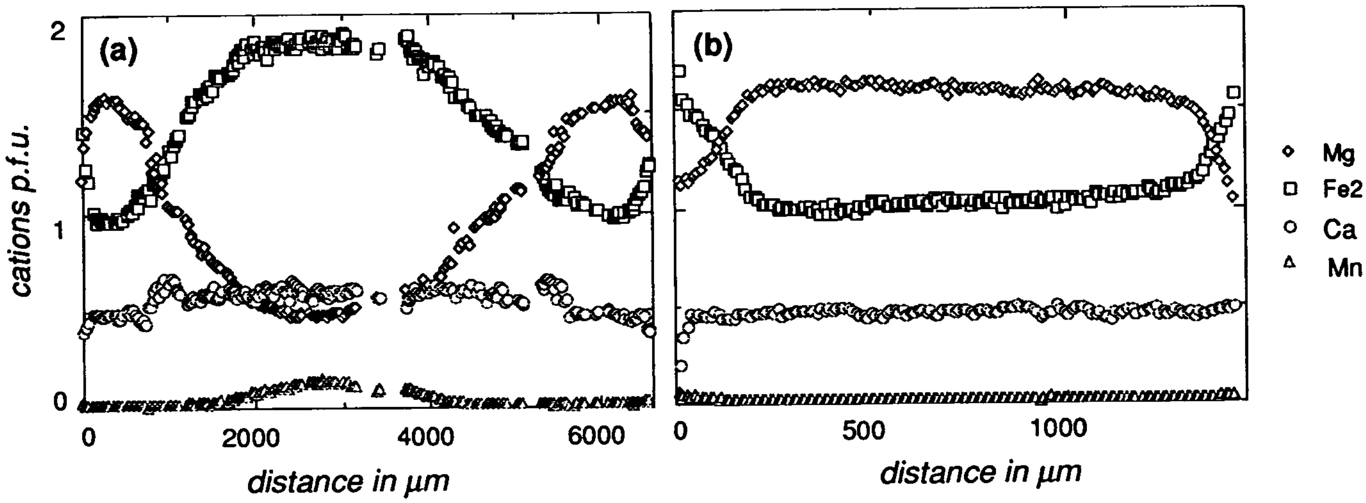

Fig. 2. Representative element concentration profiles through (**a**) large garnets and (**b**) smaller garnets of sample Z-48. Note the different scales

Garnets are rich in Fe and Ca and show zoning at their outermost rims (increasing Fe, decreasing Ca, Table 1), and they are often rimmed by radiating kelyphite of plagioclase (An_{60-70}) and hornblende. Clinopyroxene grains in the matrix (cpxI) are rather large. They have been almost completely replaced either by a fine-grained symplectite of Fe-rich diopside (cpxII) and plagioclase (An_{18-30}) or, even more often, by green amphibole (Table 1). Na_2O contents found in the cores of these grains correspond to those of clinopyroxene inclusions in garnet (1.5–2.4 wt%). Although the cores of cpxI grains are in optical continuity, their Na_2O contents have probably been lowered from their original values by retrograde transformations, as tiny plagioclase laths can be observed.

Kyanite is almost completely transformed to fine-grained coronas of hercynite, anorthite and sericite.

Metamorphic stages and thermobarometry

Temperatures for eclogites may be constrained by using geothermometers based on the distribution of Fe and Mg between garnet and clinopyroxene. Recently, several of those thermometers have either been tested empirically (Carswell and Harley 1990) or experimentally (Brey and Köhler 1990; Brey et al. 1990) and the version of Krogh (1988) turned out to yield realistic temperatures. Nevertheless, there may be significant errors in temperature estimation due to (1) extrapolation of high-temperature calibration data to lower temperatures, (2) possible effects of retrograde equilibration, (3) uncertainties in the oxidation state of Fe, especially for omphacites (4) zoning in minerals and (5) unsuitable bulk rock chemistry compared to the experimentally calibrated systems.

Minimum pressures in eclogites may be estimated by the jadeite contents of clinopyroxenes (Holland 1980) if a reasonable independant temperature estimate is available.

For breakdown phases, several thermobarometers for granulite-facies rocks may be used but are not applicable to the studied rocks. The granulite-facies reaction grt + qtz = plg + opx (+ cpx) observed in sample Z-48 only forms orthopyroxene so that no temperature estimate can be given. Pressure estimates are not reliable as there is pronounced zoning in garnet and a gradient in An contents of plagioclase between garnet and orthopyroxene. Omphacites broken down to symplectites of plg + cpx + opx, as present in sample Z-48, generally allow for the use of a two-pyroxene geothermometer. However, as symplectites are partly transformed to amphibole chemical equilibrium between the pyroxenes cannot be constrained.

Sample Lo-1

The high-pressure assemblage grt + cpxI preserved in this rock allows for estimation of pressure and temperature during metamorphism.

Temperatures estimated using the thermometer of Krogh (1988) show only a very modest pressure dependence of $\pm$ 2.5°C/0.1 GPa. On assuming a reasonable minimum pressure (confirmed by estimation of minimum pressures from X_{jad} in cpxI, see below), application of this thermometer to garnet cores and omphacite cores as well as to garnets and inclusions of omphacite in the latter gives:

$$T(°C) = 672 \pm 50 \text{ (assumed P = 1.6 GPa, n = 42)}$$

Using the thermometers on garnet rims and omphacite rims (matrix) yields

$$T(°C) = 734 \pm 52 \text{ (assumed P = 1.4 GPa, n = 22)}$$

The temperature rise suggested between cores and rims of garnets and clinopyroxenes is to be taken with caution as cpxI rims have partly been altered to cpxII and garnet composition is the same in cores and rims.

Minimum pressures can be estimated from the jadeite contents of omphacites in quartz-bearing assemblages using the experimental data of Holland (1980). The eclogite Lo-1 contains no free quartz, but plagioclase within symplectites formed from omphacites may point to its former existence. Taking X_{jad} in omphacite cores and in cpxI inclusions in garnet as 0.39 and using the temperature of 672°C deduced above gives minimum pressures of about 1.5–1.6 GPa. CpxI rims have X_{jad} of 0.22 and yield pressures of 1.3–1.4 GPa at temperatures around 734°C. Symplectite clinopyroxenes (cpxII) show only negligible contents of Al and Na and increasing Tschermaks substitution compared to cpxI. Hence, X_{jad} in cpxI cores, cpxI rims and cpxII indicates clinopyroxene evolution under falling pressures.

Sample Z-48

The metamorphic evolution of sample Z-48 is rather complex and P-T conditions can only roughly be estimated due to lacking preservation of suitable mineral assemblages.

Prograde and peak metamorphic stages

The first metamorphic stage recorded is that indicated by staurolite inclusions in garnet, mantled by pargasite. These staurolites are most likely relics of a garnet-forming reaction (e.g. st + qtz = grt + ky) as kyanite is present in the matrix and as rare inclusions in garnet and as X_{Mg} values of staurolite decrease towards garnet. Staurolites now observed in garnet were probably prevented from reacting out by the absence of quartz in direct contact, as suggested by the presence of tiny spinel grains in staurolite and in the surrounding pargasite. The possibility that staurolite formed by a retrograde reaction from garnet and kyanite as for axample reported by Enami and Zang (1988) is very unlikely as (1) there are kyanite inclusions preserved in garnet and (2) kyanite breakdown products in garnet and in the matrix are the same and consist of spinel and plagioclase rather than of staurolite.

Mg contents of staurolite cores are fairly high (up to 4.9 wt%). Experimental studies on staurolite show that the Mg endmember is only stable above 11 kb at 750°C (Schreyer 1968) in quartz-free systems, whereas Fe-staurolite is stable down to 0.1 GPa (Richardson 1968) and Fe-staurolite + quartz react to form almandine and kyanite at minimum pressures of 0.9 GPa and temperatures of about 700°C (Ganguly 1972). These findings suggest a strong pressure and temperature-dependence of Mg contents in staurolite. A strong pressure dependence seems to be further affirmed by the compilation of Ballèvre et al. (1989), showing that in medium-pressure rocks, staurolite is always richer in Mg than garnet, whereas the reverse holds true for high-pressure rocks. Staurolites compositionally similar to those of this study were experimentally obtained from mafic compositions at 2.4–2.6 GPa and 740-760°C (Hellman and Green 1979) and have been found in metamorphic rocks for which pressures and temperatures of 0.7–0.8 GPa and 800°C (Schreyer et al. 1984, peraluminous silica-deficient rocks) as well as 1.2 GPa and 750°C (Ward 1984, metatroctolites) have been constrained. All these relationships suggest high P-T conditions for the formation of the garnet cores of sample Z-48.

Peak metamorphic conditions in the rock were reached with formation of the assemblage ky + omph + grt + qtz. As there are kyanite inclusions in garnet cores and inner rims, both domains should represent the high-pressure stage of metamorphism. X_{jad} for omphacites in sample Z-48 cannot be determined as omphacites have completely broken down to symplectites. Minimum pressures for the assemblage jad_{50} + ky + H_2O are around 2.0 GPa at 700°C (Holland 1979).

Garnets that retain their zoning patterns record changes in growth conditions and may thus allow for a qualitative estimation of the P-T loop. Based on the experimental results of Råheim and Green (1974), Brey and Köhler (1990), and on modeling results of Loomis and Nimick (1982) and Loomis (1982), declining Fe/Mg ratios in conjunction with bell-shaped Mn profiles as observed in the large garnets of sample Z-48 (except from the outermost rims) may be interpreted as reflecting rising temperatures from core to rim during prograde growth. On the other hand, the scale of zoning in these garnets argues for a rapid change in the garnet-forming reaction in addition to changing P-T conditions, followed by diffusional readjustment of element distribution between the garnet cores and the inner rims as suggested by the smoothly curved concentration lines. This would imply an originally even steeper concentration gradient which is still recorded by the discontinuity (abrupt rimward decrease) within the Ca profiles, probably due to the sluggishness of Ca diffusion (Loomis et al. 1985).

The facts that garnets smaller than about 2 mm are not zoned (except from their outermost rims) and compositionally correspond to the inner rims of the large garnets suggest that they began to grow later than large garnets and all formed by the same garnet-forming reaction that also produced the inner rims of the large garnets. The possibility that small garnets started to grow at the same time as the cores of the large garnets and were subject to diffusive relaxation after growth (limited postcrystalline diffusion, Jiang and Lasaga 1990), is less likely. Firstly, diffusion velocities for Mg and Fe in garnet are rather low and the garnets were not subject to any long lasting period of HT-LP overprint after growth (see discussion). Secondly, the idea would imply that also the inner rims of the large garnets were completely readjusted by diffusion which is rather unlikely because of the extreme differences in element contents between cores and inner rims.

In conclusion, the zoning patterns of the large garnets can be explained by a single metamorphic event during which P, T and the garnet-forming reaction changed. The cores and inner rims of the large garnets and very likely also the small garnets grew under prograde and peak metamorphic conditions which can roughly be estimated at 1.0–2.0 GPa and about 750°C.

Breakdown stages

The pargasite grains in garnet which may contain inclusions of staurolite and spinel are no true inclusions in garnet but grew at a later stage of metamorphism. This is concluded from the facts that (1) pargasites grew over cracks which cut through garnet and staurolite, (2) these cracks are filled with fine-grained retrograde phases, indicating transport of chemical components, (3) pargasites

Table 2. Results of Sm–Nd analyses

Sample:	Sm (ppm)	Nd (ppm)	147 Sm/144 Nd	143 Nd/144 Nd	E_{Nd} (462 Ma)
Lo-1 wr	2.329	5.521	0.2551±03	0.512695±07	−2.3
Lo-1 grt AL	2.263	0.995	1.3763±11	0.515175±46	
Lo-1 cpx L	1.870	6.980	0.1620±01	0.512495±09	
Z-48 wr	2.147	5.682	0.2285±02	0.512521±21	−4.2
Z-48 wr rep	2.228	6.081	0.2215±46	0.512541±14	
Z-48 grt	1.725	3.625	0.2876±01	0.512742±24	
Z-48 grt L	1.178	1.864	0.3823±05	0.512991±16	
Z-48 grt ir AL	1.150	0.340	2.0430±63	0.516527±22	
Z-48 grt c AL	1.653	0.569	1.7558±43	0.515946±26	
Alp-1 wr	3.322	12.737	0.1576±03	0.512582±15	1.2
Alp-1 grt AL	2.437	1.040	1.4180±27	0.515324±82	

Abbreviations: grt: garnet, c: core, ir: inner rim, cpx: clinopyroxene, wr: whole rock, rep: full replicate analysis, L: leached, A: abraded

are also associated with quartz inclusions or do not show any intergrowths at all.

Further breakdown features are (1) the formation of coronas of spinel and anorthite from kyanite, (2) the reaction grt + qtz = plg + opx (+ amph), documenting granulite-facies conditions and (3) the formation of kelyphites of plagioclase, gedrite and in cases spinel from garnet and (4) the formation of gedrite from pargasite (and garnet). The first three transformations are probably coupled as formation of the coronas surrounding kyanite requires supply of Fe, Mg and Ca. The outermost rims of all garnet grains also record the growth of retrograde mineral phases from garnet. Due to the formation of plagioclase and amphibole and/or orthopyroxene, Ca contents and X_{Mg}-values in garnets decrease towards the rims. With breakdown proceeding, amphiboles grew at the expense of symplectites and kelyphites. The last overprint is the fluid-induced formation of biotite, sometimes intergrown with plagioclase, quartz and sillimanite.

Sample Alp-1

As primary clinopyroxene grains of sample Alp-1 (cpxI) are chemically heterogeneous and have been retrogressed to a large degree, no reasonable pressure estimate can be given. Temperatures estimated on the base of the thermometer of Krogh (1988) using cpxI inclusions in garnet and cpxI cores from the matrix must therefore also be taken with caution. Temperatures assuming the same pressures as for sample Lo-1 are

$T(°C) = 684 \pm 45$ (assumed $P = 1.6$ GPa, $n = 24$)

Geochronology

Sm-Nd analyses were carried out on all samples described above in order to date eclogite-facies metamorphism. Rb-Sr analyses were performed on suitable breakdown phases, only present in sample Z-48, to gain information on the timing of retrogression. Sample Z-48 bears zircons which were isotopically analysed for U and Pb to possibly constrain the formation of the precursor rocks to the eclogites.

Sm-Nd dating

Figure 3 shows Sm-Nd isochron diagrams with the data points for analysed mineral and whole rock fractions from the three samples discussed above. The analytical results for the single data points are listed in Table 2. Within error limits, the calculated isochron ages for all three samples are identical.

For eclogite Lo-1 isotopic equilibrium at 337 ± 6 Ma between grt, cpx and the whole rock sample can clearly be deduced as all points fall on the isochron. This is to be expected as apart from minor phases cpx and grt constitute the whole rock and as the whole rock has not been significantly altered by retrogression.

In sample Z-48, no primary omphacite is preserved. Thus, only garnets and a whole rock sample were analysed. No well-defined isochron can be calculated for all data points. The data points corresponding to the whole rock sample and a full replicate analysis of the latter clearly fall below the reference line calculated for all data points (Fig. 3d). Isotopic equilibrium between garnet and whole rock was either never attained or disturbed during retrogression. Both are probably the case as the rock is heterogeneous on a very small scale and retrogression is very pronounced in the eclogitic parts. Calculating the reference line only for garnet data points leads to an isochron displaying the same age within the error limits (334 ± 11 Ma) as the reference line. Isochrons calculated separately for grt c AL and grt ir AL with fractions grt and grt L also yield the same ages within these error limits.

The positions of data points for variably processed garnet separates within the isochron diagram yield information on Sm and Nd concentrations and isotope ratios within the analysed grains (Table 2). The data point for the garnet fraction that was neither leached nor abraded (grt) lies very close to the whole rock point and shows similar Sm and Nd concentrations as well as isotope ratios. Leached but non-abraded garnets (grt L) have

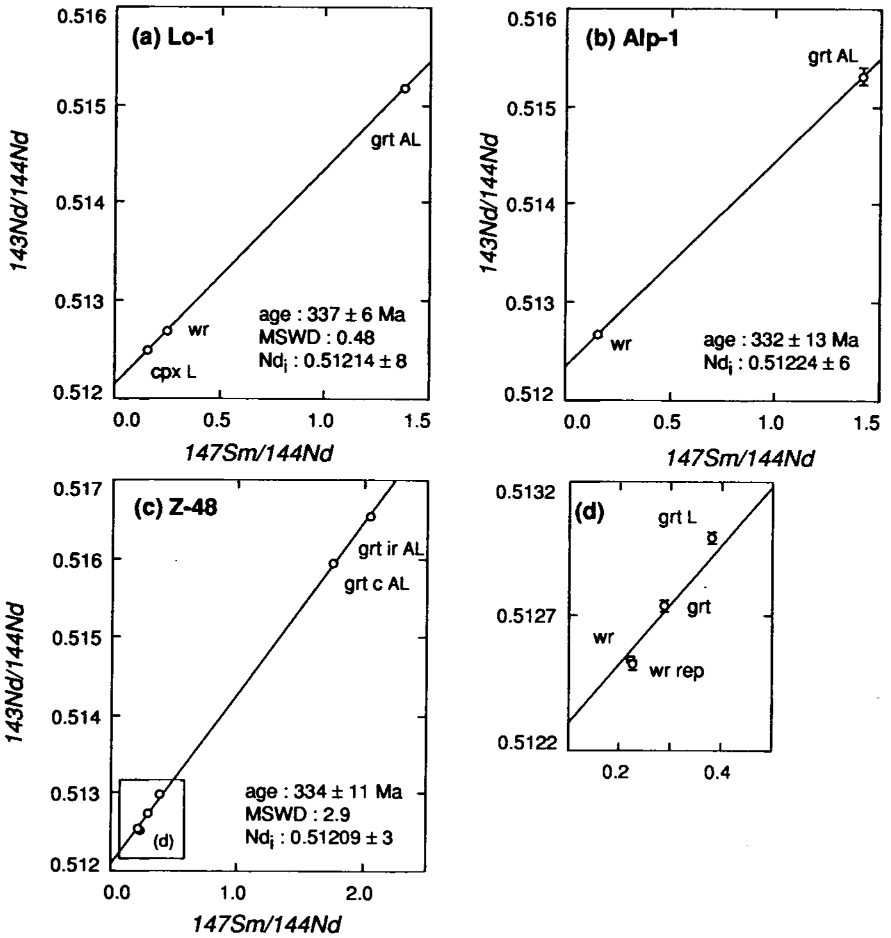

Fig. 3. Sm-Nd isochron diagrams for garnet, clinopyroxene and whole rock fractions of samples Lo-1 (**a**), Alp-1 (**b**) and Z-48 (**c-d**). Where no error bars for the points are shown the errors are too small to be adequately presented on the diagram scales. All quoted errors on isochron ages are 2σ errors, except for sample Alp-1 where the error was estimated a-priori from the errors of the two single data points. Abbreviations: *grt*: garnet, *c*: core, *ir*: inner rim, *cpx*: clinopyroxene, *wr*: whole rock, *rep*: full replicate analysis, *L*: leached, *A*: abraded. Calculated ages for sample Z-48:
334 ± 11 Ma (all data points);
328 ± 6 Ma (all garnet data points);
327 ± 8 Ma (grt, grt L, grt ir AL);
330 ± 10 Ma (grt, grt L, grt c AL)

slightly higher $^{147}Sm/^{144}Nd$ ratios and lower element concentrations. Abraded and leached garnet cores (grt c AL) and garnet inner rims (grt ir AL) show considerably higher, but varying $^{147}Sm/^{144}Nd$ ratios and very low element abundances. These relationships indicate that (1) fractions grt c AL and grt ir AL which are not affected by retrogression features record the true Sm-Nd isotope ratios and element abundances for garnet; (2) different $^{147}Sm/^{144}Nd$ ratios and element concentrations in garnet cores and inner rims correspond to the pronounced zoning in Mg, Fe, Mn and Ca; (3) the outermost retrogressed rims which are included in the leached grt L fraction obviously exchanged Sm and Nd with adjacent phases after growth as they show lower $^{147}Sm/^{144}Nd$ ratios and Sm and Nd concentrations than the cores and inner rims; (4) the grt separate obviously contains whole rock material, concentrated at the garnet rims.

Only one garnet and one whole rock fraction from sample Alp-1 were analysed for Sm-Nd isotope ratios and element abundances as primary clinopyroxenes are very heterogeneous and have been replaced by retrograde symplectite and amphibole to a large degree. The garnet-whole rock reference line yields an age of 332 ± 13 Ma which is consistent with the mineral isochron ages obtained for the other two samples.

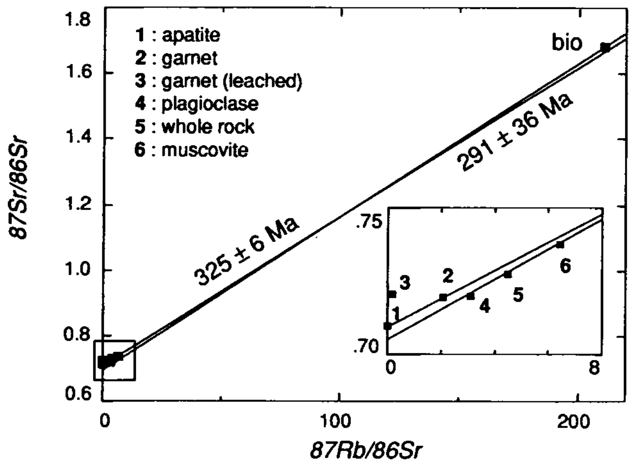

Fig. 4. Rb-Sr isochron diagram for retrograde mineral phases, garnet and whole rock of sample Z-48. The error on the 291 Ma line calculated with all data points (MSWD = 55, Sr_i = 0.7096 ± 13) corresponds to 2σ while the error for the line calculated through whole rock and biotite data points (325 Ma, Sr_i = 0.7065) was estimated a-priori from the errors on the two single data points. For further explanation see text

Table 3. Results of Rb—Sr analyses

Sample	Rb (ppm)	Sr (ppm)	$^{87}Rb/^{86}Sr$	$^{87}Sr/^{86}Sr$
Z-48 wr	111.4	71.74	4.502±01	0.72729±04
Z-48 bt	256.7	3.863	210.6±03	1.68052±55
Z-48 ms	30.98	13.96	6.44±16	0.73742±05
Z-48 ap	1.695	278.5	0.01761±05	0.70996±03
Z-48 plg	277.3	258.5	3.107±26	0.71984±07
Z-48 grt	3.055	4.224	2.095±01	0.71973±18
Z-48 grt L	0.1941	2.902	0.1937±04	0.72053±11

Abbreviations: wr: whole rock, bt: biotite, ms: muscovite, ap: apatite, plg: plagioclase, grt: garnet, L: leached

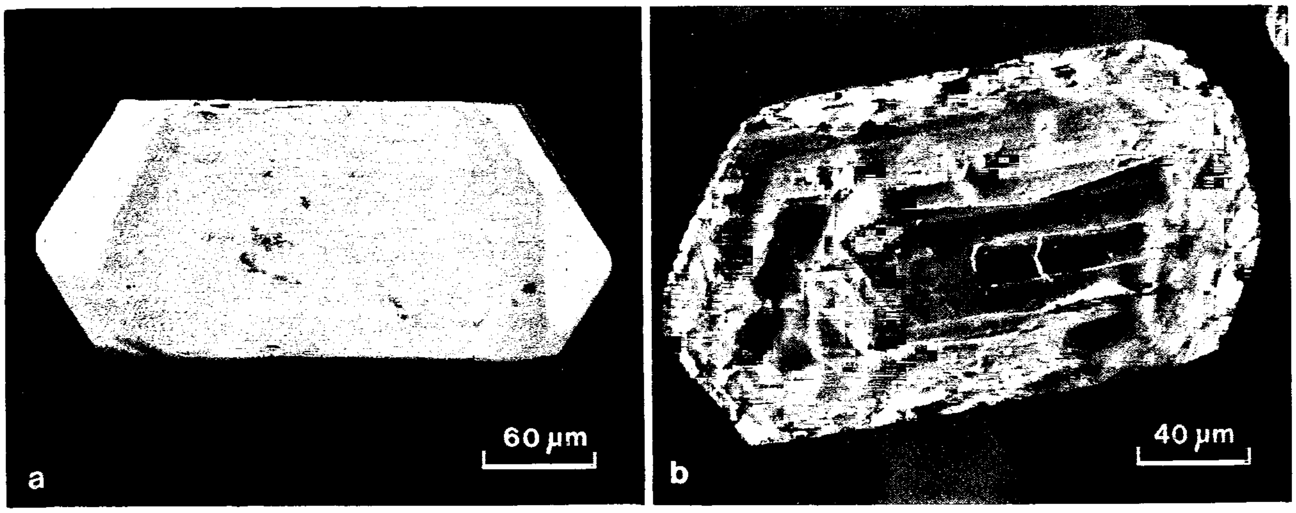

Fig. 5. SE-photograph (a) and cathode-luminescence photograph (b) of typical euhedral zircon grains from sample Z-48

Rb-Sr dating

Figure 4 shows the results of Rb-Sr dating of retrograde phases (biotite, muscovite, plagioclase) as well as apatite, garnet and whole rock from sample Z-48. The fact that no true isochron can be calculated is due to (1) heterogeneity of the sample, (2) the presence of strongly retrogressed parts within the rock, (3) different closure temperatures for the analysed mineral phases (compare Giletti 1991) and, (4) non-equilibration between the Rb-Sr systems of mineral phases. The latter especially holds true for garnet. From the positions of the data points for leached garnet (grt L) and untreated garnet (grt) in Fig. 4 and from Table 3 it can clearly be deduced that Rb and Sr contents as well as the $^{87}Rb/^{86}Sr$ ratio were significantly lowered in garnet by leaching while at the same time the $^{87}Sr/^{86}Sr$ ratio slightly increased. This suggests that point 2 represents a mixture of garnet and whole rock material whereas point 3 corresponds to the garnet Rb-Sr isotope system proper which obviously did not equilibrate with the rest of the phases.

From the reasons detailed above, no geological significance is ascribed to the 291 Ma reference line calculated with all data points (Fig. 4). More importance is attached to the 325 Ma reference line between whole rock and biotite as the slope of the line is controlled by the high $^{87}Rb/^{86}Sr$ ratio of the biotite. The 325 Ma line therefore most likely approximates the age of biotite growth, i.e. the time of low-pressure high-temperature overprint.

U-Pb dating on zircons

The zircon features of sample Z–48 differ from those commonly shown by metabasic eclogites. The zircon contents are very high, grain sizes range up to more than 500 µm and almost all zircon grains show a distinct elongation (Fig. 5a). Zircon grains up to 250 µm in size are clear, colourless prismatic crystals which are either euhedral or show slightly rounded edges. The larger zircons (300–500 µm) are prismatic, slightly pink-coloured crystals. Cathode-luminescence observations on zircons of various grain sizes reveal complex internal structures. Most grains have a dark, faintly luminescent core area showing distinct zoning and a strongly luminescent rim of variable width (Fig. 5b).

Figure 6 shows a detail of the U-Pb concordia diagram with the data points for all analyzed multigrain zircon fractions and single zircons. There is no strictly systematic relationship between grain size, U contents

Table 4. Results of U–Pb analyses on zircons of sample Z-48

Fraction (µm)			Weight (mg)	U (ppm)	Pb (ppm)	Measured ratios (IC)			Calculated ratios[b]		Age (Ma)*
						$^{208}Pb/^{206}Pb$	$^{207}Pb/^{206}Pb$	$^{206}Pb/^{204}Pb$	$^{206}Pb/^{238}U$	$^{207}Pb/^{235}U$	$^{207}Pb/^{206}Pb$
1	40–60	euhedral	1.270	1011.6	82.81	0.348627±42	0.067711±06	1241 ±01	0.06633±14	0.5124±12	450.7
2	40–60	rounded	1.174	826.4	60.96	0.280473±89	0.067258±61	1272 ±63	0.06293±03	0.4841±32	444.2
3	40–60	euh+rd	0.603	1195.8	95.84	0.329573±99	0.075206±30	771 ±18	0.06504±18	0.5049±31	464.4
4	60–100	euhedral	0.891	899.3	75.26	0.33957 ±53	0.073920±49	819 ±05	0.06743±07	0.5216±18	456.4
5	60–100	euhedral L	2.473	829.5	60.37	0.287131±36	0.061168±07	2724 ±21	0.06236±10	0.4799±15	445.2
6	60–100	rounded	0.639	742.7	53.31	0.24578 ±38	0.070333±50	1004 ±67	0.06287±05	0.4839±48	445.1
7	60–100	rounded L	2.236	698.4	49.77	0.246189±27	0.060712±05	2762 ±46	0.06315±01	0.4827±06	430.0
8	100–150	euhedral	1.796	824.6	66.90	0.311214±57	0.071594±07	929.3±6.5	0.06696±02	0.5161±16	448.4
9	100–200	euh+rd L	1.445	717.5	50.44	0.244606±24	0.063883±20	1769 ±47	0.06197±18	0.4755±18	438.2
10	150–250	rounded	0.867	608.0	44.65	0.26279 ±15	0.080808±72	568 ±48	0.06278±17	0.477 ±99	416.3
11	>500	2 crystals euh L[a]	0.238	205.9	11.84	0.13399 ±19	0.10211 ±13	302.6±5.5	0.05356±48	0.3999±84	377.6
12	>500	1 crystal euh L[a]	0.161	200.3	11.83	0.15599 ±41	0.10938 ±27	270 ±2.2	0.05516±71	0.425 ±18	448.8
13	<500	2 crystals euh abraded[a]	0.163	241.2	12.26	0.07097 ±53	0.07607 ±54	625 ±93	0.0516 ±14	0.376 ±23	322.7

Abbreviations: L: leached, [a] measured at the laboratory in Mainz, [b] calculations according to the procedure given by Ludwig (1980)

and degree of discordancy (Fig. 6, Table 4), due to the complex internal structure of most of the zircon grains. By leaching for the purpose of eliminating the strongly luminescent rims, U and Pb contents, "common Pb" as well as $^{207}Pb/^{235}U$ ratios and $^{207}Pb/^{206}Pb$ ages were lowered (compare the positions of the data points for fractions 4, 5 and 6, 7, respectively, in Fig. 6). This relationship indicates the absence of older, inherited zircon cores. Despite their large errors, the positions of the data points corresponding to large abraded zircons (13) and to large non-abraded zircons (11, 12) also clearly show that the faintly luminescent cores of the zircons bear no distinctly older, inherited Pb component. From the positions of the data points both for leached and abraded zircon grains and for non-treated zircon fractions it must be concluded that the strongly luminescent rims of the zircons are overgrowths which are richer in U and Pb and therefore bear more radiogenic Pb than the cores.

No discordia can be calculated for all zircon fractions. For the smaller grain size fractions a discordia with an upper intercept age of 462 Ma and a lower intercept age of 118 Ma can be calculated. As the lower intercept age is geologically insignificant and points to multiple Pb loss (see discussion) the upper intercept can be taken as a rough age indication only and errors on the discordia have no significance. Data points for the zircons larger than 250 µm have large errors due to small concentrations of radiogenic Pb and cluster around 325 to 350 Ma, one fraction (13) being quasi-concordant at 323 Ma.

Discussion

Interpretation of the Sm-Nd data

The interpretation of Sm-Nd isochrons on minerals and whole rock fractions of metamorphic rocks has become a matter of debate (compare Mezger et al. 1992). Especially for high-pressure rocks the questions have been put forward as to whether the Sm-Nd isochrons record peak conditions of metamorphism or rather cooling stages and as to what extent the Sm-Nd isotope system in these rocks may be affected by late-stage thermal overprint (Tilton et al. 1991; Jamtveit et al. 1992; Mezger et al. 1992; Thöni and Jagoutz 1992). From the results of these papers and from the following simple considerations it emerges that no unique but only individual interpretations of Sm-Nd isochrons on high-pressure rocks are possible:

(1) Resetting of the Sm-Nd isotope system is largely temperature and time-dependent and thus coupled with the individual P-T-t paths and absolute P-T values of the high-pressure rocks. These in turn depend on the geodynamic setting of the respective collision or subduction zones and especially on the initial positions of the rocks within them.

(2) Due to the temperature and time dependence of the isotope resetting, the peak pressure conditions of high-pressure metamorphism (e.g., maximum burial depth) can be dated only if they roughly coincide with the peak temperatures. If, on the other hand, there was a very long

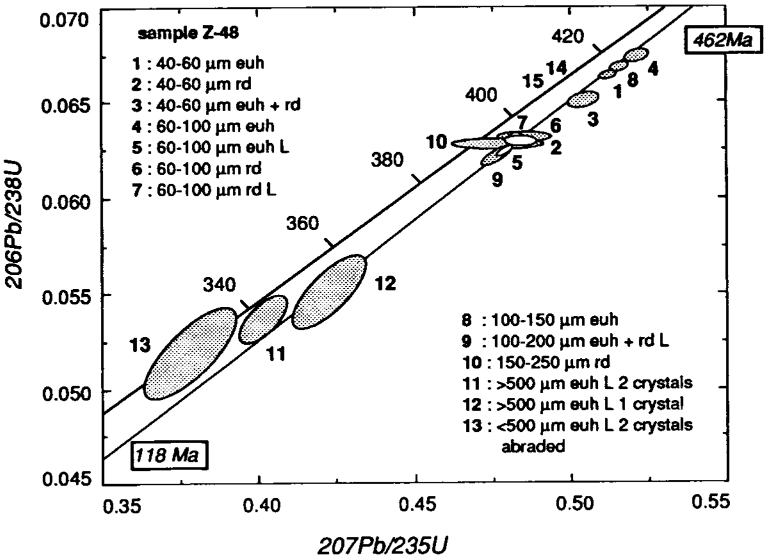

Fig. 6. Detail of the U-Pb concordia plot showing the data points for zircons of samples Z-48. Abbreviations: *L:* leached in HNO3, *euh:* euhedral, *rd:* rounded. The numbers with the zircon fractions correspond to those given in Table 4. The discordia with an upper intercept of 462 Ma and a lower intercept of 118 Ma was calculated with zircon fractions 1–10. No errors are assigned to these intercept ages as the lower intercept is geologically meaningless (see text)

period of high-temperature overprint subsequent to the pressure peak, or if cooling was very slow, Sm-Nd isochron ages may indeed record cooling stages.

(3) The temperature at which a mineral in a rock becomes closed with respect to a decay system is dependent on parameters such as grain size, cooling rate, diffusion velocities and coexisting mineral phases (Dodson 1979; Giletti 1991). Therefore, a unique closure temperature for the Sm-Nd system in high-pressure rocks cannot exist.

Based on the considerations detailed above and on the geological situation, there are two main points to be discussed for the studied samples: (1) The extent to which the Sm-Nd isotope system could have been affected by the Carboniferous LP-HT metamorphism which the host rocks of the eclogites have experienced. If the petrological data do not constrain a severe, long lasting period of high-temperature overprint subsequent to burial of the rocks, the Sm-Nd isochron ages record high-pressure metamorphism. (2) The connection of P-T data to the isochron ages. Linking P-T data to Sm-Nd isochron ages is in general afflicted with the problem that geothermometers based on the distribution of main elements may record temperatures that do not necessarily coincide with the time given by the Sm-Nd chronometer, as diffusion velocities for Sm and Nd in garnet and clinopyroxene (Harrison and Wood 1980; Sneeringer et al. 1984) will most probably differ from those of main elements (Elphick et al. 1985; Cygan and Lasaga 1985; Sautter et al. 1988; Chakraborty and Ganguly 1992) and are only poorly constrained.

In sample Lo-1, garnet and clinopyroxene grains are chemically homogeneous and show no zoning (except for the outermost rims of matrix cpxI), indicating equilibrium conditions for main elements between the two minerals at the end of their growth. This chemical homogeneity cannot be explained by diffusive readjustment of main elements during a temperature rise after the pressure peak as X_{jad} of matrix cpxI grains still record evolution at falling pressures, and as a temperature rise cannot clearly be constrained by geothermometry and is in any case restricted to the outermost rims.

In eclogite Lo-1 there are only two major mineral phases, garnet and clinopyroxene. According to experimental results, diffusion of Al and Sm in clinopyroxene (Freer et al. 1982; Sneeringer et al. 1984; Sautter et al. 1988) is slower than diffusion of Fe, Mg, and Sm in garnet (Harrison and Wood 1980; Elphick et al. 1985; Loomis et al. 1985). Therefore, clinopyroxene has a higher closure temperature for Sm, and garnet becomes closed to the Sm-Nd exchange as soon as the clinopyroxene closure temperature is reached. Although it cannot be constrained that the equilibrium temperature of approximately 672°C, recorded by Fe-Mg distribution between garnet and clinopyroxene, corresponds to the closure temperature for the Sm-Nd system in clinopyroxenes of eclogite Lo-1, it emerges from the experimental data that the clinopyroxene closure temperature cannot have been lower than 672°C, as no experiments showing diffusion of Sm to be faster than diffusion of main elements is known so far. Therefore, garnet and clinopyroxene growth at peak metamorphic conditions, (i.e. maximum burial depth) is recorded by the Sm-Nd isochron age.

For sample Z-48, interpretation of the Sm-Nd data is more complex as there are more than two phases and as large garnets are zoned in major and trace elements. Based on the considerations detailed in the section on metamorphic evolution and thermobarometry, it was concluded that the garnets show only very limited diffusional and retrograde features. It was further deduced that zoning patterns of large garnets record two stages of a high-pressure metamorphic event, corresponding to two different garnet-forming reactions. The cores of large garnets grew at the first stage, whereas their inner rims and very likely also the small garnets grew at the second stage.

The two different garnet fractions (grt c AL and grt ir AL) corresponding to these two growth stages yield the same isochron ages when calculated separately. This clearly shows that the garnets grew rather rapidly within the time span indicated by the error on the Sm-Nd isochron. Thus, the two metamorphic stages recorded by garnet zoning, including the P_{max}-stage, are not resolvable from each other as they were passed too quickly. A similar result has been obtained by Vance and O'Nions (1990) by Sm-Nd studies on very large garnets of metapelitic rocks from Newfoundland.

Garnets of sample Alp-1 are not zoned (except from their outermost rims) and temperatures estimated are in the range of those calculated for sample Lo-1, suggesting that element distribution in these garnets still records peak metamorphic growth conditions. The Sm-Nd isochron age (garnet and whole rock) coincides with the two well-defined mineral isochrons. It is therefore taken as recording high-pressure metamorphism, although an interpretation of isotope data on the base of information from mineral data is hampered by retrograde transformations of cpxI.

Zircon data

U-Pb analyses on multigrain zircon fractions from most metamorphic rocks lead to discordant data points in the concordia diagram. These do not yield unequivocal age information as (1) there are no petrologic constraints on the growth conditions of accessory phases like zircons, (2) in the case of meta-igneous rocks, zircons may be of magmatic and/or of metamorphic origin, (3) zircons may be partly or entirely inherited from external sources, (4) growth or overgrowth of $ZrSiO_4$ as well as U and Pb loss may occur during different metamorphic stages or events at different P-T conditions. Additionally, the mechanisms of Pb loss in zircons are not very well known, a handicap to the proper interpretation of lower intercept ages on zircon discordias in general. Proposed mechanisms are episodic Pb-loss (Wetherill 1956), leading to geologically significant lower intercepts, as well as diffusional (Tilton 1960) and multi-episodic Pb loss (Wetherill 1963), both resulting in geologically meaningless lower intercepts.

Morphology and internal structure of zircons in eclogites are commonly used to decide whether they are of magmatic or metamorphic origin (Peucat et al. 1982; Gebauer et al. 1985). Zircons of samples Z-48 are mainly euhedral and elongated grains displaying regular zoning and lacking inherited cores (Fig. 5). These features point to a magmatic formation. The upper intercept ages of the discordias therefore very likely reflect magmatic zircon crystallization. From the arrangement of the data points from sample Z-48 in the concordia plot and from the geologically insignificant lower intercept age a simple model for episodic Pb loss must be rejected. Pure diffusional lead loss must also be excluded as there is no simple correlation between grain size and discordancy, due to overgrowth of rims. The zircons smaller than 250 μm which set up the discordia for Z-48 have obviously experienced recent lead loss, as indicated by the lower intercept. It is not clear whether they also experienced partial lead loss in the Carboniferous, as indicated by the position of the data points for zircons > 250 μm. During high-pressure metamorphism temperatures were probably below about 750°C (see section on thermobarometry) and the U-Pb system of zircons may survive extreme P-T conditions in some cases (e.g. Gebauer et al. 1988; Claoué-Long et al. 1991). On the other hand, the large, nearly concordant zircons obviously either experienced almost total lead loss or they grew at about 323 Ma, corresponding to the time of high-pressure metamorphism within the error limits of the U-Pb data.

In any case, the zircon data indicate multistage zircon growth and mixing of several Pb components, implying that the Ordovician upper intercept age only roughly approximates magmatic crystallization of the small zircon grains. The age may be taken as the magmatic formation of the precursor rocks of the eclogites if the zircons were formed "in situ". This cannot be clearly constrained for sample Z-48 as (1) zircon contents and Zr abundances are very high compared with those of modern basaltic rocks, (2) bulk rock composition (strong enrichment in Al, deficiency in Si and Ca) points to a basaltic precursor rock that has experienced weathering or other alteration prior to metamorphism, (3) $^{87}Sr/^{86}Sr$ ratios and ε_{Nd} values calculated for 462 Ma B.P. point to the contribution of a crustal component, and (4) it has been shown that the U-Pb system of zircons can even be unaffected when the zircons are taken up by melts (Gebauer et al. 1988).

Geological implications

The only radiometric datum on high-pressure rocks in the Schwarzwald that has been published so far is the $^{207}Pb/^{206}Pb$ age of a single zircon (Pb evaporation technique) from a metabasic granulite with high-pressure mineral relics (341 ± 19 Ma), suggesting that high-pressure metamorphism and granulite-facies overprint of metabasites are of Carboniferous age (Hanel et al. 1993).

From other Variscan areas, Devonian ages of HP metamorphism have been reported (Stosch and Lugmair 1990; Carswell and Jamtveit 1991; Beard et al. 1992) but there is also an increasing number of Carboniferous ages of HP metamorphism. Sm-Nd isochron ages of 323–342 Ma on garnet, clinopyroxene and whole rock samples of garnet-pyroxenites, garnet peridotites and eclogites from the Gföhl unit in Czechoslovakia (Beard et al. 1991, 1992) constrain a HP event. Sm-Nd isochron ages between 324 and 352 Ma have been obtained from eclogites of the Szieznik Massif, Polish Sudetes and of the Moldanubian zone of the Bohemian Massif (Brückner et al. 1991). Though interpreted as cooling stage, a Sm-Nd isochron age of 344 ± 10 Ma is reported for a garnet pyroxenite from the Moldanubian zone of Lower Austria (Carswell and Jamtveit 1991). Although these rocks come from different structural units within the Variscan belt and despite the fact that no clear correlation of structural units between the Bohemian Massif and the Schwarzwald has been attempted up to now, the Sm-Nd isochron ages clearly constrain a Carboniferous collisional event followed by crustal thickening for some parts of the Variscan orogen.

For the Schwarzwald geochronological studies were also carried out on the LP-HT gneisses and migmatites encompassing the eclogites and reveal the main metamorphic event (LP-HT) in the Schwarzwald to have occurred between 329 and 336 Ma B.P. (Kalt et al. 1993).

Comparing the Sm-Nd isochron ages for high-pressure metamorphism with the ages for LP-HT metamorphism of the surrounding gneisses and migmatites shows that on using realistic error calculations the two stages or events cannot clearly be distinguished from each other by conventional dating techniques. This is in detail corroborated by comparison of the Sm-Nd data (isochron age: 334 ± 11 Ma) and the Rb-Sr data (whole rock - biotite age: 325 ± 6 Ma) obtained on sample Z-48 in this study with the U-Pb ages of monazites from the directly adjacent migmatite (330 ± 1 Ma, Kalt et al. 1993). A similar situation is found in Lower Austria where ages of HP metamorphism (344 ± 10 Ma, Carswell and Jamtveit 1991) seem to coincide with the age of granulite-facies metamorphism (Schenk and Todt 1983).

Apart from the insufficient resolution of the different dating techniques used and apart from the possibly anisochemical retrogression of the whole rock samples, a reason for the coincidence of ages may be the fact that metamorphic processes can operate on time scales not resolvable by conventional dating techniques (Zeitler 1989; Vance and O'Nions 1990). Geochronological studies using different conventional dating methods on (high-pressure) metamorphic rocks in collision zones have constrained a very rapid decompression and uplift (e.g. Stosch and Lugmair 1990; Zeck et al. 1992). These findings are further corroborated by tectonic studies and models of subduction and collision zones which offer tectonic mechanisms for rapid unroofing of collisional belts and exhumation of high-pressure rocks (Platt 1986; Hsü 1991; Little et al. 1992).

U-Pb zircon ages similar to the Ordovician upper intercept age found in this study have been obtained from other metamorphic rocks of the Schwarzwald, namely from meta-igneous gneisses (Todt and Büsch 1981), from migmatites (Steiger et al. 1973; Kober 1987), and from metasedimentary gneisses (Kober 1986). Ordovician upper intercept ages of discordias from zircons have also been found for various metamorphic rocks of other Variscan areas (Gebauer et al. 1981; Pin and Lancelot 1982). All these zircon data are difficult to interpret due to the lack of petrological control on zircon growth, but they point to magmatic and/or metamorphic events in the Early Paleozoic.

Conclusions

Petrological and geochronological studies on three eclogite samples from the Schwarzwald yield the following results concerning the P-T-t evolution of the rocks.

(1) The eclogites experienced minimum pressure conditions of 1.6 GPa and peak temperatures between 672 and 750°C.

(2) The age of high-pressure metamorphism is recorded by Sm-Nd isochron ages of 332 ± 13 Ma, 334 ± 11 Ma and 337 ± 6 Ma on garnet, clinopyroxene and whole rock.

(3) Reaction textures in all three eclogites and prograde growth zoning in large garnets of one sample (Z-48) record subsequent metamorphic stages. The first prograde stage is documented by rare staurolite inclusions in garnet cores of one eclogite. The peak high-pressure mineral assemblage is grt + cpx ± ky ± qtz ± rt. Retrograde breakdown of the high-pressure phases grt and cpxI can be described by the reactions grt + qtz = plg + opx and cpxI (+ qtz) = cpxII + plg ± opx. Further retrogression leads to formation of amphibole.

(4) Reaction textures and garnet zoning patterns in conjunction with the Sm-Nd data of one sample (Z-48) indicate that garnets must have grown during a rather short period of several Ma as their cores and rims record overlapping Sm-Nd isochron ages.

(5) Exhumation of the high-pressure rocks was also rather fast as constrained by a Rb-Sr isochron age of 325 ± 6 Ma on retrograde biotite and whole rock. Due to rapid exhumation and insufficient resolution of the age data, the HP stage of metamorphism cannot clearly be distinguished from the later LP-HT stage which the eclogites share with their country rocks.

(5) Ordovician upper intercept ages of discordias on zircons in conjunction with their morphology are a rough estimate of the magmatic crystallization age and indicate that zircons may survive high-grade metamorphism without being completely reset.

Appendix

Analytical techniques

Mineral analyses were performed using a Camebax SX 50 microprobe equipped with 4 spectrometers. Operating parameters were: 20 s counting time (15 s for Na, K), 10 nA beam current and 15 kV accelerating voltage. PAP correction was applied to the data. Natural and synthetic oxide and silicate standards were used for calibration.

For isotope analyses, whole rock powders and mineral separates were obtained from about 0.5 kg sample material. Larger samples were used for extraction of zircons. After crushing and sieving minerals were concentrated by conventional magnetic and specific gravity separation techniques. Micas were further purified by repeated grinding in alcohol and sieving. All mineral separates were handpicked from grain size fractions of 100–150 µm. For sample Z-48, the large cm-sized garnets were deliberately crushed in order to enable separation of reddish-coloured fragments corresponding to the cores from pink-coloured fragments corresponding to the inner rims. To remove the outermost retrograde rims, garnets from all samples were abraded (Krogh 1982) after handpicking (except fractions "grt" and "grt L" from sample Z-48) and subsequently checked again for purity under a binocular microscope. All mineral separates were leached in a H_2O/HNO_3-mixture (except micas and fraction grt from sample Z-48), cleaned ultrasonically, and dried with ultrapure acetone.

Mineral separates for Sm-Nd and Rb-Sr analyses were digested in teflon screw top containers by a HNO_3/HF-mixture after adding $^{149}Sm/^{146}Nd$ and $^{87}Rb/^{84}Sr$ spike solutions, respectively. Rb, Sr, and REE were extracted on quartz glass columns using a cation exchange resin and HCl. For samples Z-48 and Alp-1, Sm and Nd were separated on cation exchange columns by α-Hiba. For sample Lo-1, Sm and Nd were separated by reverse chromatography using teflon powder coated with 2-ethyl hexyl phosphoric acid. Sm-Nd isotope analyses for samples Alp-1 and Z-48 were performed on a single collector NBS-designed TELEDYNE mass spectrometer at the Zentrallabor für Geochronologie, University of Münster. Nd was run as NdO^+ (long-term standard values for the La Jolla standard: 0.511843 ± 6). Sm and Nd analyses for sample Lo-1 were measured on a multiple collector Finnigan MAT 261 mass spectrometer in a static mode at the Institut für Sediment- und Isotopengeologie, University of Bochum. Nd was run as metal (long-term standard values for the La Jolla standard: 0.511850 ± 5). $^{142}Nd/^{144}Nd$ ratios were normalized to 1.141739 (Lugmair and Carlson 1978). All Rb and Sr isotope analyses were carried out in Münster. A linear correction for mass fractionation was applied to $^{87}Sr/^{86}Sr$ ratios by normalizing to $^{86}Sr/^{88}Sr = 0.1194$. Measured $^{87}Sr/^{86}Sr$ ratios for NBS standard 987 were 0.710292 ± 23. Rb ratios were corrected for 0.6% fractionation per mass unit as deduced from measured values of Rb standard NBS 984 of 2.6086 ± 80. Constants used are those from Steiger and Jäger (1977) and from Lugmair and Carlson (1978). Isochron calculation follows York (1969). Quoted errors for Sr and Nd isotope ratios comprise 2σ analytical errors, uncertainties in the isotopic composition of the spike solution as well as blank corrections.

U-Pb analyses on zircons were performed at the Zentrallabor für Geochronologie in Münster and at the Max-Planck Institut für Chemie in Mainz. All zircons were washed in HNO_3 and digested by HF in teflon pressure vessels mantled by steel autoclaves. In Münster, the obtained solution was then split and a $^{235}U/^{208}Pb$ spike solution added to one aliquot for determination of concentrations (ID) while Pb isotope ratios were measured from the other part (IC). In Mainz, a $^{232}U/^{202}Pb$ spike solution was added to the whole sample. The solutions were further processed for U and Pb with anion exchange resins using standard HCl elution procedures similar to those described by Krogh (1973). In Münster, measured Pb isotope ratios were corrected for 0.012% fractionation per mass unit as deduced from measured standard values of NBS 981 ($^{204}Pb/^{206}Pb = 0.05188 \pm 28$, $^{207}Pb/^{206}Pb = 0.91372 \pm 10$, $^{208}Pb/^{206}Pb = 2.16252 \pm 44$). In Mainz, U and Pb were measured on a multiple collector Finnigan MAT 261 mass spectrometer in a static mode. Measured values for NBS standard 981 were $^{206}Pb/^{204}Pb = 16.9322 \pm 8$, $^{207}Pb/^{206}Pb = 0.914561 \pm 40$, $^{208}Pb/^{206}Pb = 2.16662 \pm 13$. The model of Stacey and Kramers (1975) was used for common lead correction. Errors as quoted in Table 4 were calculated after Ludwig (1980). The decay constants given by Steiger and Jäger (1977) were used for age calculation.

Total procedural blanks were less than 40 pg for Pb and 15 pg for U, less than 200 pg for Sr ($^{87}Sr/^{86}Sr$ ratio of blank: 0.710) and 20 pg for Rb and less than 100 pg for Sm and Nd. A blank correction was applied to the Pb data (isotopic composition of blank Pb in Münster: $^{208}Pb/^{204}Pb = 37.5$, $^{207}Pb/^{204}Pb = 15.52$, $^{206}Pb/^{204}Pb = 17.72$ and in Mainz: $^{208}Pb/^{204}Pb = 37.05 \pm 0.5\%$, $^{207}Pb/^{204}Pb = 15.59 \pm 0.5\%$, $^{206}Pb/^{204}Pb = 17.70 \pm 0.5\%$).

Acknowledgements. We would like to thank Dieter Buhl at the University of Bochum for Sm and Nd measurements. Wolfgang Todt is thanked for providing facilities for U-Pb analyses at the MPI laboratory in Mainz. We are further grateful to Hans-Peter Meyer (University of Karlsruhe) for help with the microprobe work and to Ulrich Koberski (University of Freiburg) for cathode-luminescence photographs. This study was financially supported by the Deutsche Forschungsgemeinschaft (Schl 258–1).

References

Ballèvre M, Pinardon, J-L, Kienast J-R, Vuichard J-P (1989) Reversal of Fe-Mg partitioning between garnet and staurolite in eclogite-facies metapelites from the Champtoceaux Nappe (Brittany, France). J Petrol 30:1321–1349

Beard BL, Medaris jr LG, Johnson CM, Brueckner HK, Misar Z (1991) Nd and Sr isotope geochemistry of Moldanubian eclogites and garnet peridotites, Bohemian Massif, Czechoslovakia. Terra Nova Abstract Suppl 6:4

Beard BL, Medaris jr LG, Johnson CM, Brueckner HK, Misar Z (1992) Petrogenesis of Variscan high-temperature Group A eclogites from the Moldanubian zone of the Bohemian Massif, Czechoslovakia. Contrib Mineral Petrol 111:468–483

Brey GP, Köhler T, Nickel G (1990) Geothermobarometry in four-phase lherzolites I. Experimental results from 10 to 60 kb. J Petrol 31:1313–1352

Brey GP, Köhler T (1990) Geothermobarometry in four-phase lherzolites II. New thermobarometers, and practical assesment of existing thermobarometers. J Petrol 31:1353–1378

Brewer MS, Lippolt HJ (1974) Rb-Sr age determinations of pre-tectonic granites from the Southern Schwarzwald, SW Germany. N Jb Mineral Abh 1:28–41

Brueckner HK, Medaris jr LG, Bakun-Czubarov N (1991) Nd and Sr age and isotope patterns from Variscan eclogites of the eastern Bohemian Massif. N Jb Mineral Abh 163:169–196

Carswell DA, Harley SL (1990) Mineral barometry and thermometry. In: Carswell DA (ed) Eclogite facies rocks. Blackie, Glasgow, pp 83–110

Carswell DA, Jamtveit B (1991) Variscan Sm-Nd ages for the high-pressure metamorphism in the Moldanubian Zone of the Bohemian Massif, Lower Austria. N Jb Mineral Abh 162:69–78

Chakraborty S, Ganguly J (1992) Cation diffusion in alumosilicate garnets: experimental determination in spessartine-almandine diffusion couples, evaluation of effective binary diffusion coefficients, and applications. Contrib Mineral Petrol 111:74–86

Claoue-Long JC, Sobolev NV, Shatsky VS, Sobolev AV (1991) Zircon response to diamond-pressure metamorphism in the Kokchetav Massif, USSR. Geology 19:710–713

Cygan RT, Lasaga AC (1985) Self-diffusion of magnesium in garnet at 750° to 900°C. Am J Sci 285:328–350

Dodson MH (1979) Theory of Cooling Ages. In: Jäger E, Hunziker J (eds) Lectures in isotope geology. Springer, New York Berlin Heidelberg, pp 194–202

Eisbacher GH, Lüschen E, Wickert F (1989) Thrusting and extension in the Hercynian Schwarzwald and Vosges, Central Europe. Tectonics 8:2–21

Elphick SC, Ganguly J, Loomis TP (1985) Experimental determinations of cation diffusivities in alumosilicate garnets. Contrib Mineral Petrol 90:36–44

Enami M, Zang Q (1988) Magnesian staurolite in garnet-corundum rocks and eclogite from the Donghai district, Jiangsu province, east China. Am Mineral 73:48–56

Flöttmann T, Kleinschmidt G (1989) Structural and basement evolution in the Central Schwarzwald Gneiss Complex. In: Emmermann R, Wohlenberg J (eds) The German Continental Deep Drilling Program (KTB). Springer, Berlin Heidelberg New York, pp 265–275

Franke W (1989) Variscan plate tectonics in Central Europe – current ideas and open questions. Tectonophysics 169:221–228

Freer R, Carpenter MA, Long JVP, Reed SJB (1982) "Null result" diffusion experiments with diopside: implications for pyroxene equilibria. Earth Planet Sci Lett 58:285–292

Ganguly J (1972) Staurolite stability and related parageneses: theory, experiment, and applications. J Petrol 13:335–365

Gebauer D, Bernard-Griffiths J, Grünenfelder M (1981) U-Pb Zircon and monazite dating of a mafic-ultramafic complex and its country rocks. Contrib Mineral Petrol 76:292–300

Gebauer D, Lappin M, Grünenfelder M, Wyttenbach A (1985) The age and origin of some Norwegian eclogites: a U-Pb zircon and REE study. Chem Geol 52:227–247

Gebauer D, Von Quadt A, Compston W, Williams IS, Grünenfelder M (1988) Archean zircons in a retrograded Caledonian eclogite of the Gotthard massif (Central Alps, Switzerland). Schweiz Mineral Petrogr Mitt 68:485–490

Giletti BJ (1991) Rb and Sr diffusion in alkali feldspars, with implications for the cooling histories of rocks. Geochim Cosmochim Acta 55:1331–1343

Hanel M, Lippolt HJ, Kober B, Wimmenauer W (1992) Lower Carboniferous granulites in the Schwarzwald basement near Hohengeroldseck (SW-Germany). Die Naturwissenschaften 1/93:25–28

Harrison WJ, Wood BJ (1980) An experimental investigation of the partitioning of REE between garnet and liquid with reference to the role of defect equilibria. Contrib Mineral Petrol 72:145–155

Hellman PL, Green TH (1979) The high pressure experimental crystallization of staurolite in hydrous mafic compositions. Contrib Mineral Petrol 68:369–372
Hofmann A, Köhler H. (1973) Whole rock Rb-Sr-ages of anatectic gneisses from the Schwarzwald, SW-Germany. N Jb Mineral Abh 119:163–187
Holland TJB (1979) Experimental determination of the reaction paragonite = jadeite + kyanite + H_2O, and internally consistent thermodynamic data for part of the system Na_2O - Al_2O_3 - SiO_2 - H_2O, with applications to eclogites and blueschists. Contrib Mineral Petrol 68:293–301
Holland TJB (1980) The reaction albite = jadeite + quartz determined experimentally in the range 600–1200°C. Am Mineral 65:129–134
Hsü KJ (1991) Exhumation of high-pressure metamorphic rocks. Geology 19:107–110
Jagoutz E (1988) Nd and Sr systematics in an eclogite xenolith from Tanzania: evidence for frozen mineral equilibra in the continental lithosphere. Geochim Cosmochim Acta 52:1285–1293
Jamtveit B, Carswell DA, Mearns EW (1991) Chronology of the high-pressure metamorphism of Norwegian garnet peridotites/pyroxenites. J Metam Geol 9:125–139
Jiang J, Lasaga AC (1990) The effect of post-growth thermal events on growth-zoned garnet: implications for metamorphic P-T history calculations. Contrib Mineral Petrol 105:454–459
Kalt A, Grauert B, Baumann A (1993) Rb-Sr and U-Pb studies on migmatites from the Schwarzwald (FRG): evidence for incomplete isotopic resetting during high-temperature metamorphism. J Metam Geol, manuscript in revision
Klein H, Wimmenauer W (1984) Eclogites and their retrograde transformation in the Schwarzwald (FRG). N Jb Mineral Mh 1:25–38
Kober B (1986) Whole-grain evaporation for 207Pb/206Pb-age investigations on single zircons using a double filament thermal ion source. Contrib Mineral Petrol 93:482–490
Kober B (1987) Single-zircon evaporation with Pb^+ emitter bedding for 207Pb/206Pb-age investigations using thermal ion mass spectrometry, and implications to zirconology. Contrib Mineral Petrol 96:63–71
Krogh EJ (1988) The garnet-clinopyroxene Fe-Mg geothermometer – a reinterpretation of existing experimental data. Contrib Mineral Petrol 99:44–48
Krogh TE (1973) A low-contamination method for hydrothermal decomposition of zircon and extraction of U and Pb for isotope determination. Geochim Cosmochim Acta 37:485–494
Krohe A, Eisbacher GH (1988) Oblique crustal detachment in the Variscan Schwarzwald, Southwestern Germany. Geol Rundsch 77:25–43
Little TA, Holcombe RJ, Gibson GM, Offler R, Gans PB, McWilliams O (1992) Exhumation of late Paleozoic blueschists in Queensland, Australia, by extensional faulting. Geology 20:231–234
Loomis TP, Ganguly J, Elphick SC (1985) Experimental determination of cation diffusivities in aluminosilicate garnets. II. Multicomponent simulation and tracer diffusion coefficients. Contrib Mineral Petrol 90:45–51
Loomis TP (1982) Numerical simulation of the disequilibrium growth of garnet in chlorite-bearing aluminous pelitic rocks. Canad Mineral 20:411–423
Loomis TP, Nimick FB (1982) Equilibrium in Mn-Fe-Mg aluminous pelitic compositions and the equilibrium growth of garnet. Canad Mineral 20:393–410
Ludwig KR (1980) Calculation of uncertainties of U-Pb isotope data. Earth Planet Sci Lett 46:212–220
Lugmair GW, Carlson RW (1978) The Sm-Nd history of KREEP. In: Proc 9th Lunar Planet Conf, Geochim Cosmochim Acta, pp 684–704
Mehnert KR, Büsch W (1982) The initial stage of migmatite formation. N Jb Mineral Abh 145:211–238
Mezger K, Essene EJ, Halliday AN (1992) Closure temperatures of the Sm-Nd system in metamorphic garnets. Earth Planet Sci Lett 113:397–409
Mørk MBE, Kullerud K, Stabel A (1988) Sm-Nd dating of Seve eclogites, Norrbotten, Sweden-Evidence for early Caledonian (505 Ma) subduction. Contrib Mineral Petrol 99:344–351
O'Brien PJ (1989) The petrology of retrograded eclogites of the Oberpfalz Forest, northeastern Bavaria, West Germany. Tectonophysics 157:195–212
O'Brien PJ, Carswell DA, Gebauer D (1990) Eclogite formation and distribution in the European Variscides. In: Carswell DA (ed) Eclogite facies rocks. Blackie, Glasgow, pp 204–224
O'Brien PJ, Röhr C, Okrusch M, Patzak M (1992) Eclogite facies relics and a multistage breakdown in metabasites of the KTB pilot hole, NE Bavaria: implications for the Variscan tectonometamorphic evolution of the NW Bohemian Massif. Contrib Mineral Petrol 112:261–278
Peucat J-J, Vidal P, Godard G, Postaire B (1982) Precambrian U-Pb zircon ages in eclogites and garnet pyroxenites from South Brittany (France): an old oceanic crust in the West European Hercynian belt? Earth Planet Sci Lett 60:70–78
Pin C, Lancelot J (1982) U-Pb dating of an early Paleozoic bimodal magmatism in the French Massif Central and of its further metamorphic evolution. Contrib Mineral Petrol 79:1–12
Platt JP (1986) Dynamics of orogenic wedges and the uplift of high-pressure metamorphic rocks. Geol Soc Amer Bull 97:1037–1053
Råheim A, Green DH (1974) Experimental determination of the temperature and pressure dependence of the Fe-Mg partition coefficient for coexisting garnet and clinopyroxene. Contrib Mineral Petrol 48:179–203
Richardson SW (1968) Staurolite stability in a part of the system Fe-Al-Si-O-H. J Petrol 9:467–488
Sautter V, Jaoul O, Abel F (1988) Aluminium diffusion in diopside using the $^{27}Al(p, \gamma)^{28}Si$ nuclear reaction: preliminary results. Earth Planet Sci Lett 89:109–114
Schenk V, Todt W (1983) U-Pb Datierungen an Zirkon und Monazit der Granulite im Moldanubikum Niederösterreichs (Waldviertel). Fortschr Mineral Beih 61:190–191
Schreyer W (1968) A reconnaissance study of the system MgO-Al_2O_3-SiO_2-H_2O at pressures between 10 and 25 kba. Carnegie Inst Yearb 66:380–392
Schreyer W, Horrocks PC, Abraham K (1984) High-magnesium staurolite in a sapphirine-garnet rock from the Limpopo Belt, southern Africa. Contrib Mineral Petrol 86:200–207
Sneeringer M, Hart SR, Shimizu N (1984) Strontium and samarium diffusion in diopside. Geochim Cosmochim Acta 48:1589–1608
Stacy JS, Kramers JD (1975) Approximation of terrestrial lead isotope evolution by a two-stage model. Earth Planet Sci Lett 26:207–221
Steiger RH, Bär MT, Büsch W (1973) The zircon age of an anatectic rock in the Central Schwarzwald. Fortschr Mineral 50, Beih 3:131–132
Steiger RH, Jäger E (1977) Subcomission on Geochronology: Convention on the use of decay constants in geo- and cosmochronology. Earth Planet Sci Lett 36:359–362
Stosch HG, Lugmair GW (1990) Geochemistry and evolution of MORB-type eclogites from the Münchberg Massif, southern Germany. Earth Planet Sci Lett 99:230–249
Thöni M, Jagoutz E (1992) Some new aspects of dating eclogites in orogenic belts: Sm-Nd, Rb-Sr and Pb-Pb isotopic results from the Austroalpine Saualpe and Koralpe type-locality (Carinthia/Styria, southeastern Austria). Geochim Cosmochim Acta 56:347–368
Tilton GR (1960) Volume diffusion as a mechanism for discordant lead ages. J Geophys Res 65:2933–2945
Tilton GR, Schreyer W, Schertl HP (1991) Pb-Sr-Nd isotopic behavior of deeply subducted crustal rocks from the Dora Maira Massif, western Alps, Italy. II: What is the age of the ultrahigh-pressure metamorphism? Contrib Mineral Petrol 108:22–33
Todt W (1976) Zirkon U/Pb-Alter des Malsburg-Granits vom Südschwarzwald. N Jb Mineral Mh 12:532–544

Todt W, Büsch W (1981) U-Pb investigations on zircons from pre-Variscan gneisses - A study from the Schwarzwald, West Germany. Geochim Cosmochim Acta 45:1789–1801
Vance D, O'Nions RK (1990) Isotopic chronometry of zoned garnets: growth kinetics and metamorphic histories. Earth Planet Sci Lett 97:227–240
Ward CM (1984) Magnesium staurolite and green chromian staurolite from Fiordland, New Zealand. Am Mineral 69:531–540
Wendt I, Lenz H, Höhndorf A (1974) Alter des Bärhalde-Granites (Schwarzwald) und der Uranlagerstätte Menzenschwand. Geol Jb E2:131–142
Wetherill GS (1956) Discordant uranium-lead ages I. Trans Am Geophys Union 37:320–326
Wetherill GS (1963) Discordant uranium-lead ages II. Discordant ages resulting from diffusion of lead and uranium. J Geophys Res 68:2957–2965
Wickert F, Eisbacher H (1988) Two-sided Variscan thrust tectonics in the Vosges Mountains, northeastern France. Geodinamica Acta 2:101–120
Wimmenauer W, Klein H, Müller H, Stenger R (1989) Petrography and petrology of the KTB location Schwarzwald. In: Emmermann R, Wohlenberg J (eds) The German Continental Deep Drilling Program (KTB). Springer, Berlin Heidelberg New York, pp 244–263
Wimmenauer W, Stenger R (1989) Acid and intermediate HP metamorphic rocks in the Schwarzwald (Federal Republic of Germany). Tectonophysics 157:109–116
York D (1969) Least squares fitting of a straight line with correlated errors. Earth Planet Sci Lett 5:320–324
Zeck HP, Monié P, Villa IM, Hansen BT (1992) Very high rates of cooling and uplift in the Alpine belt of the Betic Cordilleras, southern Spain. Geology 20:79–82
Zeitler PK (1989) The geochronology of metamorphic processes. In: Daly JS et al (eds) Evolution of metamorphic belts. Geol Soc Spec Publ 43:131–148

Editiorial responsibility: J. Hoefs